

## Modelling of biological membranes and their biophysical properties

A. B. HENDRICH

*Department of Biophysics  
Wrocław Medical University  
Wrocław, Poland  
hendrich@biofiz.am.wroc.pl*

### Abbreviations:

CF - carboxyfluorescein,  
DMPC - dimyristoylphosphatidylcholine,  
MC - Monte Carlo simulation,  
MD - molecular dynamics simulation,  
PA - phosphatidic acid,  
PC - phosphatidylcholine,  
PE - phosphatidylethanolamine,  
PG - phosphatidylglycerol,  
P-gp - P glycoprotein,  
PI - phosphatidylinositol,  
SM - sphingomyelin.

### 1. Composition and structure of biological membranes

Biological membranes are present in all living cells and constitute a highly selective barrier between the cell and its surrounding as well as between different cellular compartments (nucleus, mitochondria etc.). Apart from the barrier properties membranes play also active role in metabolic, signalling and energy conversion processes. Membranes are built of two main classes of molecules: lipids and proteins. The ratio between these components depends on the type of membrane and varies from 1 : 4 up to 4 : 1 (lipid: protein, respectively). Apart from the main components membranes contain also smaller amounts of other molecules, mainly carbohydrates which are bound to lipids and proteins, forming thus glycolipids and glycoproteins, respectively.

### 1.1. Lipids

Lipids of biological membranes can be divided into several groups. Membranes of eukaryotic cells consist of three main lipid classes: phospholipids, sterols and glycolipids. Phospholipids are the most abundant in membranes and play important structural role. Due to this they are presumably the most extensively studied and the best known lipid species. The chemical structure of example phospholipid molecules: 1,2-dipalmitoyl-*sn*-glycerophosphatidylcholine and D-erythro-N-stearoyl-sphingomyelin are presented in Fig. 1.

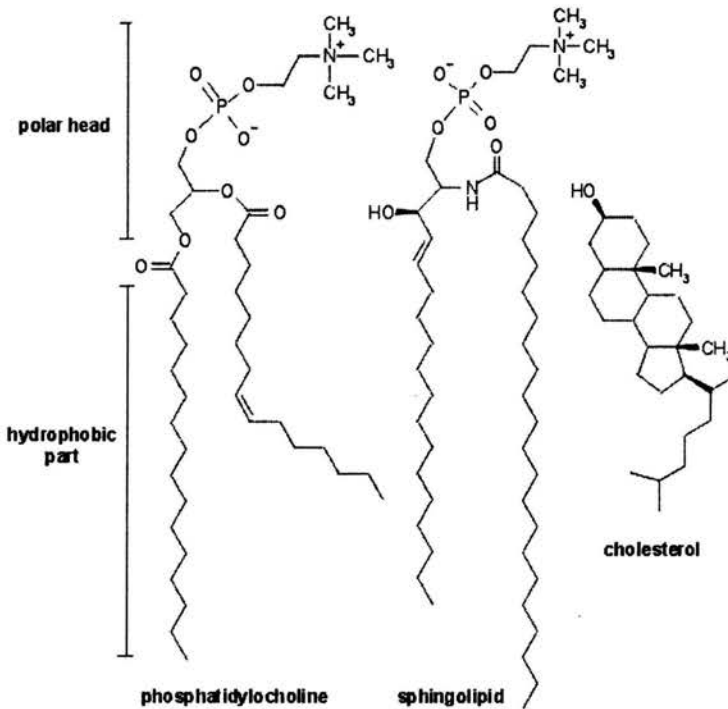


FIGURE 1. Chemical structures of some important membrane lipids: phosphatidylcholine, sphingomyelin and cholesterol.

Phosphatidylcholines and sphingomyelins are the most common among the membrane phospholipids. As it is shown in Fig. 1 phospholipid molecule consist of two different parts: polar head and hydrocarbon chains. The molecules of individual phospholipid types may differ either in the polar head group composition or by the length and degree of unsaturation of hydrocarbon chains. Depending on the chemical structure of polar group phospholipids can bear the electric charge (like negatively charged phosphatidylserine, phosphatidylglycerol or phosphatidylinositol) or be a zwitterions (like

phosphatidylcholine or phosphatidylethanolamine). Hydrocarbon chains of phosphatidylcholines usually are 14 – 18 CH<sub>2</sub> groups long and may be fully saturated or possess from one up to six unsaturated double bonds. In naturally occurring phosphatidylcholines acyl chains attached at the C1 position (left acyl chain of PC molecule in Fig. 1 called also sn-1) are usually fully saturated, while C2 (sn-2) chains are quite often unsaturated. Presence of unsaturated bond causes a “kink” in the hydrocarbon chain and thus increases the average effective space occupied by the chain (and simultaneously by a lipid molecule). Unsaturated chains, due to the presence of one (or more) double bonds are also less rigid than saturated ones.

Phospholipids of biological membranes usually possess two hydrocarbon chains, in most cases each of the same length. Asymmetric chains are present in sphingolipids – phospholipid subclass that together with phosphatidylcholines constitute more than 50% of membrane phospholipids. Typical membrane sphingolipids (see Fig. 1) contain one shorter chain (usually 18 carbon atoms long) and second much longer (20 – 24 carbon atoms). This asymmetry leads to the effects that seem to play an important structural role in membranes – recently sphingolipids were recognised as an important factor of membrane structure modulation. Some other lipid species – cardiolipins could consist of up to four hydrocarbon chains.

Cholesterol (its chemical structure is presented at the right side of Fig. 1) belongs to the group of sterols and is the most common (and thus the best studied) sterol component of eukaryotic cell membranes. Sterols are major means by which eukaryotic cells modulate membrane properties. Barrier properties of membranes as well as many other membrane physicochemical properties of lipid bilayers are strongly affected by the level of cholesterol in the membrane. Sterols with such activities are referred to as membrane-active sterols. Recently the role of cholesterol-sphingomyelin interactions in formation of membrane lipid rafts is also emphasised (see also Sec. 1.3).

Taking into account affinity to water two distinct parts of lipid molecule can be distinguished: hydrophilic polar head (see Fig. 1 - part of PC molecule containing choline and glycerol) and hydrophobic hydrocarbon chains (containing two fatty acid residues). Compounds possessing both hydrophilic and hydrophobic parts in one molecule are called amphiphiles. Apart from phospholipids also other types of membrane lipids (sterols and glycolipids) are amphiphiles. Amphiphilic character of lipid molecules is responsible for the process of their spontaneous aggregation in polar media (e.g. water) or at the polar/apolar interface. After aggregation the polar heads are directed towards water and lipid molecules form structures that prevent the contact of hydrophobic parts with polar surrounding. The example of lipid molecules organisation at air/water interface (drop of oil spread on the water surface)

is schematically shown in Fig. 2. If the number of lipid molecules at interface is sufficient they form a monolayer in which polar heads are placed on the water surface and hydrocarbon chains protrude into the air. Presence of lipid monolayer alters interactions between water molecules that are close to the surface and thus the surface tension is changed.

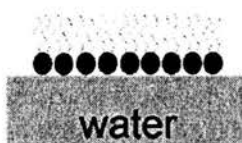


FIGURE 2. Lipid molecules spread on the water surface form monolayer.

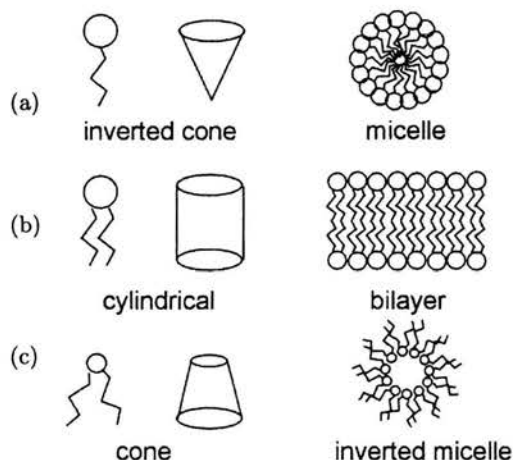


FIGURE 3. Schematic drawing of "shape concept" – the dependence between the shape of lipid molecules and type of structure spontaneously formed by them in water.

When lipid molecules are placed in a bulk water they organise themselves spontaneously into different structures. According to the "shape concept" hypothesis the effective shape of lipid molecule (i.e. the space occupied by the molecule after the hydration of its polar part) is one of the most important factors governing the type of structure formed [3, 17]. The idea of "shape concept" is presented in Fig. 3. As can be seen, generally three types of lipid molecule shapes are distinguished: inverted cone, cylindrical and cone. In the inverted cone-like molecules the space occupied by polar heads is much greater than space occupied by hydrophobic part and therefore those molecules will spontaneously form micellar or hexagonal ( $H_I$ ) structures (Fig. 3a).

Cylindrical molecules are likely to form bilayers (lamellar structures usually denoted by letter  $L$ ) in which the average area occupied by polar and hydrophobic parts are equal. Hydrophobic part of cone-like molecules occupies greater area than its polar part and such a molecules form inverted micellar or hexagonal ( $H_{II}$ ) structures. Micellar and bilayer structures are common in biological systems and their role is well established, but inverted structures are not often met in cellular systems and their role is discussed. It seems, however, that inverted structures play some role as intermediate stages of membrane fusion – a process in which two membranes join together and form one membrane. Fusion processes are of great importance when considering the events happening during the fertilization or viral attack on the host cell.

The idea of shape concept has been formalised by introduction of an index called critical packing parameter (cpp) [14]. This parameter describes the ratio of the areas packing by acyl chains and polar heads and is defined as:

$$\text{cpp} = \frac{V_h l_c^{-1}}{a_0}, \quad (1.1)$$

where  $V_h$  is a volume of hydrocarbon chains,  $l_c$  - the length of chains in extended position, and  $a_0$  - the area occupied by molecule. Taking into account the above definition we obtain that when  $\text{cpp} < 0.5$  then molecules are cone shaped, for  $0.5 < \text{cpp} < 1.0$  molecules should be considered as cylinders and for  $\text{cpp} > 1.0$  molecules are inverted cones.

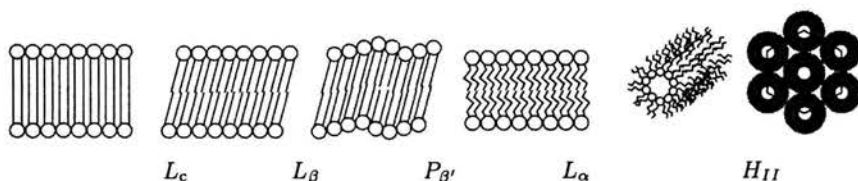


FIGURE 4. Basic types of phases existing at different temperatures.  $L_c$  - crystalline,  $L_\beta$  - gel,  $P_{\beta'}$  - rippled,  $L_\alpha$  - liquid crystalline,  $H_{II}$  - inverted hexagonal.

Temperature and amount of water present in the system are additional factors determining which particular form of structure is adopted by lipid molecules. Since in biological system water is in most cases present in excess the role of sample hydration will be omitted in this paper. The role of temperature is clearly seen when considering the type of phospholipid packing in bilayers. Depending on the temperature and type of phospholipid molecules several different phases (kinds of lipid packing) exist in bilayers and non-bilayer structures. These phases are schematically presented in Fig. 4,

where  $L_c$  (lamellar crystalline) is the lowest temperature phase and subsequent phases could appear as the temperature of lipid system is raised. As it is presented, each phase is characterised by different packing of both hydrocarbon chains and polar heads of lipids. As a consequence of different polar heads packing the hydration of bilayer surface (access of water molecules to the polar region) is altered in each phase. Certain phases differ also in the motional freedom of hydrocarbon chains – they are immobilised and rigid in  $L_c$  phase, and almost fluid in  $L_\alpha$  or  $H_{II}$  phases. The transitions from one phase to another are the first order transitions and several bilayer properties are abruptly changed along with the phase change. To these parameters belong among others: volume, thickness and area of lipid bilayer, specific heat capacity, electric properties like capacity or conductivity. Phospholipid phase transitions can be thus detected by several physical methods, among them calorimetry and different types of spectroscopy to name the most common techniques used in lipid phase properties investigations.

It is important to emphasize that presumably none of phospholipids could adopt all of the presented in Fig. 4 modes of molecular packing. Taking into account some of the best known phospholipids: phosphatidylcholines can be organized in  $L_c$ ,  $L_\beta$ ,  $P_\beta$  and  $L_\alpha$  phases, while phosphatidylethanolamines for example can be packed in  $L_\beta$ ,  $L_\alpha$  and  $H_{II}$  structures. All phospholipids, however, could form  $\beta$ -type ( $L_\beta$  and some also  $P_\beta$ ) and  $L_\alpha$  phases and therefore transition between  $\beta$ -type and  $L_\alpha$  phases is called main phase transition. During this transition the most dramatic changes of bilayer structure (and simultaneously almost all bilayer parameters) take place – hydrocarbon chains “melt” and also packing of polar head groups is altered. Melting of hydrocarbon chains means that instead of being in *trans* conformation they also adopt *gauche* conformation what enables them to move more freely. On the other hand phases listed in Fig. 4 does not contain a full set of different structures that can be formed by hydrated lipids. Those structures, however, are not of great importance for biological systems and therefore can be skipped in this short description.

## 1.2. Proteins and peptides

Generally the topic of protein structure and function is extremely wide and at least partial description of this problem is far out of the scope of this article. I will focus here exclusively on membrane proteins and those of their properties which are crucial for different aspects of bilayer structure which are discussed in this paper. Membrane proteins should be either attached to the surface of membrane (peripheral proteins) or embedded into the lipid bilayer (integral proteins).

Peripheral proteins are anchored to the membrane by the electrostatic interactions with charged lipids or by binding to the integral proteins. In last years an important way of anchoring was found for so called GPI (glycosylphosphatidylinositol) anchored proteins. To put it briefly a GPI anchored protein is a proteolipid molecule which uses the phosphatidylinositol hydrocarbon chains to bind to the surface of membrane. Peripheral proteins weakly interact with the membrane lipid phase and therefore their influence on the membrane properties is relatively small but in most cases cannot be neglected.

Integral proteins penetrate the hydrophobic core of lipid bilayer and to do this they must possess in their structure also some hydrophobic fragments or domains. Usually such protein domains are spatially organised in form of  $\alpha$ -helices or hydrophobic  $\beta$ -barrels. To fit properly to the hydrocarbon region of membrane hydrophobic domains of proteins should have proper size – this problem is known in literature as “protein-lipid hydrophobic matching” [15]. According to this model any kind of hydrophobic mismatch introduces a mechanical stress into membrane and should result in different effects: from protein lateral segregation up to the change of cell shape. Apart from perturbation of membrane hydrophobic part integral proteins could interact also with the polar heads of lipids. Both types of interactions could affect the structure of membrane and thus alter its biophysical properties [19].

Peptides, like their “big brothers” – proteins, are build of amino acids and depending on their sequence should be hydrophobic, hydrophilic or amphiphilic. A general difference between proteins and peptides is in their size – the last ones being much smaller than the previous. The main consequence

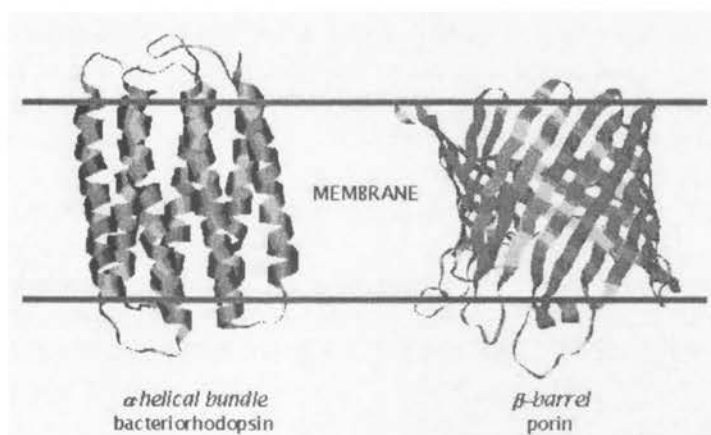


FIGURE 5. The most often met structures of protein hydrophobic domains –  $\alpha$ -helix and  $\beta$ -barrel.

of size difference is that integral peptides might diffuse in the plane of membrane much faster than proteins. Fast lateral diffusion plays an important role in the formation of temporal ionic channels by gramicidin molecules (gramicidin is an antibiotic).

### 1.3. Structure of biological membranes

The concept of the role and structure of biological membranes has evolved from the static bilayer playing the role of passive, homogeneous barrier between the cell and its surrounding [8] up to the fluid, asymmetric and heterogeneous mosaic, actively contributing to the processes of mass, energy and information exchange [26] (and further, continuous modifications). All of the models, however, use as a basic membrane structure the same type of lipid molecules spatial arrangement – the lipid bilayer.

Fluidity is very often recognised as the most striking feature of biological membranes; however, the precise definition of this “parameter” is discussed and not perfectly clear. Generally membrane fluidity means that all membrane components are highly mobile and they have different degrees of motional freedom. Single molecules are usually not rigid – their parts can oscillate and rotate, as an example can serve here the movements of hydrocarbon chains of lipid in liquid-crystalline phase. Whole molecules are also free to move along the membrane surface (so called lateral diffusion) and rotate (rotational diffusion). Lipid molecules can also “jump” from one membrane leaflet to another – this kind of movement is called flip-flop. All these motions cause that biological membranes are dynamic and due to this many of structures formed within membrane should be treated as temporal, but not permanent complexes. Membrane fluidity (or motions of membrane components) could be assessed by many experimental techniques – different spectroscopic methods like IR, fluorescence, EPR, NMR are the most convenient in this purpose.

Fluidity of eukariotic cell membranes strongly depends on the amount of cholesterol. Molecules of this sterol easily incorporate into the lipid bilayers and in specific way modulate their properties. In model membranes – consisting of phosphatidylcholines or phosphatidylethanolamines – cholesterol increases fluidity of gel phase, but reduces fluidity of liquid-crystalline phase. In natural membranes at higher concentrations (> 25 – 30 mol%) cholesterol induces new modes of membrane molecular packing – so called liquid ordered and liquid disordered phases [2]. It is generally believed that cells regulate the permeability and fluidity of their membranes due to the control of cholesterol content.



According to our present knowledge membranes are asymmetric – it means that both lipid and protein content of each of membrane leaflets is different. In eukaryotic cells outer membrane leaflet is usually rich in neutral phospholipids like phosphatidylcholines and sphingomyelins. Simultaneously the outer surface of membrane is poor in peripheral proteins – almost exclusively a GPI-anchored proteins are attached to this side. Negatively charged lipids (like phosphatidylserines) are present in the inner – cytosolic – layer of the membrane. Peripheral protein content of this membrane layer is also bigger – among others the membrane skeleton proteins are attached to this side. Lipid asymmetry of membrane is maintained by the processes of active transport and biochemical reactions like synthesis and degradation of certain membrane lipid components.

As a consequence of described above membrane asymmetry a bilayer couple hypothesis was proposed to explain the molecular mechanism of the erythrocyte shape changes resulting from the action of different drugs [24]. Erythrocytes are devoid of any intracellular structures (apart from the membrane skeleton) and therefore are extremely susceptible to the shape changes induced by different factors. Depending on the type of drug used erythrocytes could pass through a series of shapes which usually finish in one of the final forms: echinocyte or stomatocyte (Fig. 6).

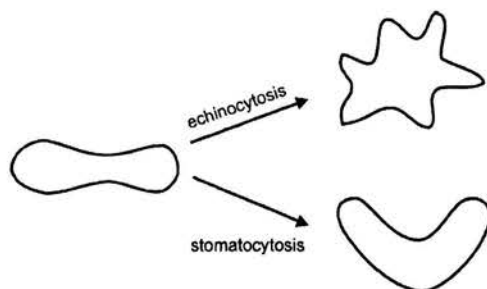


FIGURE 6. Stomatocytic and echinocytic transformation of the erythrocyte shape.

According to the bilayer couple hypothesis drugs causing the shape changes interact preferentially with only one of the bilayer leaflets and the type of final erythrocyte shape depends on which layer is the target (Fig. 7). If the cytoplasmic side of the membrane is preferred by the drug molecules expansion of this layer causes the invagination of membrane and erythrocyte stomatocytosis is observed. Since the cytoplasmic side of erythrocyte membrane contains negatively charged lipids it is expected that this leaflet will be preferred by cationic drugs that can penetrate membrane and thus are amphiphilic. If the outer side of membrane is preferentially occupied by drug

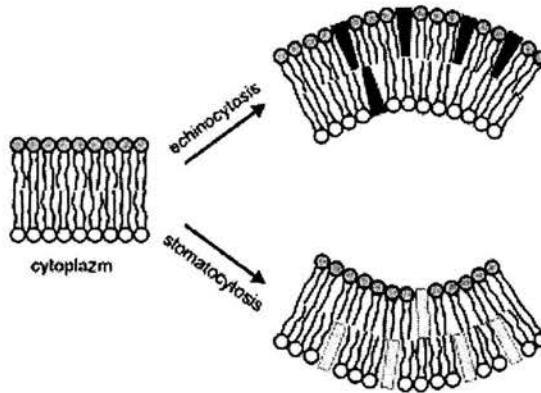


FIGURE 7. Bilayer coupling results in deformation of the membranes.

molecules the echinocytosis effect is observed. The echinocytosis and stomatocytosis can be also described in terms of positive and negative membrane curvature effects. The molecules incorporated into the outer membrane layer induce positive membrane curvature, while the molecules preferring intercalation into inner layer cause negative curvature effects. To make the picture more realistic it is worth to emphasise that bilayer couple hypothesis effects should be considered in parallel with the shape concept effects. Since most of the molecules interacting with membranes hardly could be considered as cylinder-shaped, the expansion of certain region of inner or outer membrane layers must be taken into consideration.

In recent years a special attention is paid to the problem of membrane heterogeneity. The fact that membranes are heterogeneous, i.e. the composition of different regions laying in the plane of membrane is not identical, was known since many years. In the past decade, however, it appeared that this lateral segregation of membrane components presumably plays an important role in the functions carried out by membranes. In several types of cells existence of membrane microdomains called lipid rafts was confirmed [13, 24]. The major components of lipid rafts are sphingolipids and cholesterol, which in model systems were proved to segregate spontaneously and form separate domains [4]. Apart from lipid components rafts consist also of certain kinds of proteins which are responsible for raft functions and/or structure. Lipid rafts containing protein called caveolin form invaginations in the membrane – *caveole*. Presence of rafts and *caveole* was found in many cell types, mostly in tissues involved in the transport processes: epithelial and from blood-brain barrier. Schematic drawing of lipid raft and *caveole* is presented in Fig. 8. Lipid rafts and *caveole* are supposed (or in some cases already

proved) to play an important role in membrane-related processes like endocytosis, mechanotransduction, lipid transport and signal transduction [5, 18].

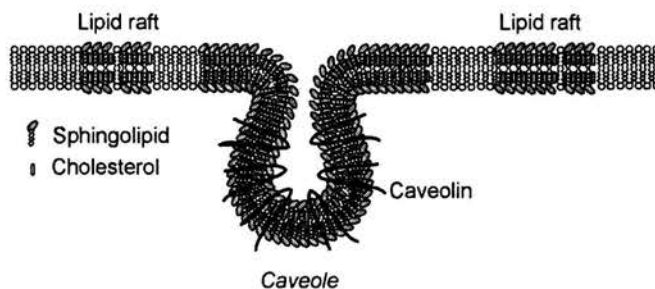


FIGURE 8. Schematic presentation of lipid raft (left and right) and *caveole* (in the middle).

## 2. Experimental models

The general aim of biophysical research is to elucidate the physical background of processes occurring in biological systems. Due to the high complexity of biological objects this aim is very often approached by the studies performed on model systems, which are less sophisticated than living cells and enable a reasonable description by only a limited set of variables. Biophysical modelling is performed on two levels: experimental and theoretical.

Using synthesised or purified and well characterised components, scientists are able to construct experimental models, which at least partially mimic certain parts of the cell or tissue. These models enable to follow the behaviour of original objects using less or more sophisticated experimental techniques. Studies performed on experimental models provide us the knowledge of the most basic rules governing the behaviour of living systems.

On the other level the theoretical models are constructed to describe and predict the properties of certain systems or subsystems. Since most of the theoretical models could not describe the very complex living systems they usually focus on the properties of experimental models. Taking this into account one can conclude that experimental models are used not only because they mimic living systems but also because they serve as a link between theory and real life. For this reason apart from some theoretical models described in the last part of this article, also a few of the most often used experimental model systems will be described along with some examples of their applications.

## 2.1. Multilamellar systems

Multilamellar systems are produced by dispersing lipids in aqueous media. They can be obtained very easily by shaking lipid in a sufficient amount of water (or buffer) at temperature above the main phase transition. Due to the described above propensity of lipids for self-organization in aqueous media and in accordance with shape concept, bilayer structures are formed spontaneously by cylinder-like molecules. If amount of lipid is high enough single bilayers stack one over another and multilamellar structure appears. Such a systems are used for the studies of lipid phase behaviour, structure of bilayers and influence of different factors on lipid thermotropic properties and structure.

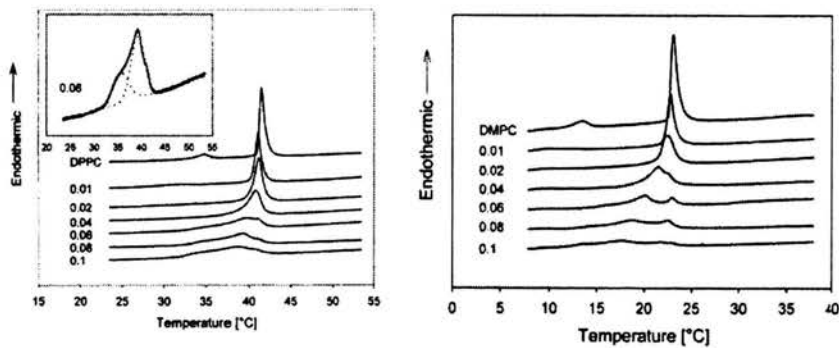


FIGURE 9. Thermograms of dipalmitoyl (left) and dimyristoylphosphatidylcholine (right) with increasing amounts of trifluoperazine. In the insert the deconvolution of the double peak is shown. Figures are taken from [11].

The investigation on the influence of trifluoperazine on the thermotropic behaviour of phospholipids [11] will serve as an example of study performed using multilamellar systems. Trifluoperazine is a phenothiazine derivative and is used in clinics as an antipsychotic drug. It was also found that trifluoperazine can act as drug modulating multidrug resistance of cancer cells (for multidrug resistance see also Sec. 2.3). Since one of the possible mechanisms of the multidrug resistance modulation involves the lipid phase of membrane, the influence of trifluoperazine on the thermotropic properties of some phospholipids was studied. The behaviour of phospholipid multilamellar structures formed with the addition of the studied drug was investigated using microcalorimetry. The thermograms obtained for mixtures of dipalmitoyl- and dimyristoylphosphatidylcholine with increasing amounts of trifluoperazine are shown in Fig. 9. As presented in this figure the maxima of transition profiles (corresponding to the temperature of lipid main

phase transition) were shifted towards lower temperatures as the amount of drug in mixtures increased. Additionally for both of the studied lipids at trifluoperazine: lipid molar ratios higher than 0.04 (dipalmitoylPC) and 0.06 (dimyristoylPC) in thermograms presence of two overlapping transition peaks was observed. Thermograms containing two overlapping peaks were deconvoluted into separate components (as presented in the inset of left part of Fig. 9). Presence of multiple transition peaks instead of one is usually interpreted as appearance of phase separation in the studied system. Separation of phases in trifluoperazine: PC systems was confirmed by other experiments but since they were performed on unilamellar liposomes they will not be described in this section. Appearance of phase separation was attributed to the different ionisation states (protonated or deperotonated) in which trifluoperazine could exist in experimental conditions. Each form could slightly differently interact with phospholipid and this could lead to phase separation. Analysis of other thermodynamic data that are obtained from thermograms (like enthalpy change during the transition) revealed that trifluoperazine molecules after incorporation into bilayers locate at the polar/apolar interface of membrane.

## 2.2. BLMs

Black (or Bilayer) Lipid Membranes are often used in the studies of the electrical properties of lipid bilayers. The typical way of BLM formation is to put a drop of lipid dissolved in an organic solvent (butanol for example) on a small hole in a Teflon support placed in an aqueous media (Fig. 10). After the evaporation of organic solvent the lipid drop forms a single bilayer in the central part of the hole, what is observed by microscope as blackening of the hole area (that's where the name BLM comes from). BLM's can be also formed on the tip of micropipette immersed in aqueous media.

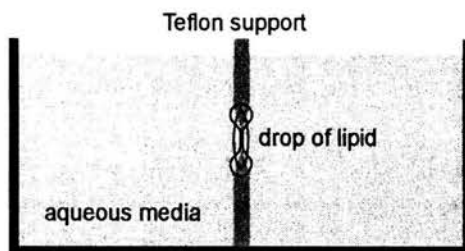


FIGURE 10. Black lipid membrane formed on the hole in the Teflon support. Dashed line shows the shape of lipid drop, solid line corresponds to the shape of BLM (in the central part of the hole).

Usually the experimental BLM set-up apart from Teflon support and water (buffer) container consist also of electromotive force source, two electrodes located in the compartments divided by BLM and an electric current meter. Using such experimental set-up it is possible to perform the measurements that enable to prepare  $I - V$  (current-voltage) characteristics of BLM's and to calculate the electric resistance (or in certain cases also capacitance) of membranes.

The study on the translocation of alkali metal cations by lipophilic cyclodextrin derivatives through bilayer membranes [16] will be described below as an example of BLM model application.

One of the mechanisms of antibiotics biological activity is transport of cations through the cellular membranes carried out by the antibiotic molecules. Ion transport could be performed in two ways: through the channel formed in membrane by antibiotic molecules (case of gramicidin) or by carrying the ions across the membrane by other antibiotics (case of valinomycin). The ion-carriers form a complex with an ion, transport it and finally release ion on the opposite side of membrane (see Fig. 11).

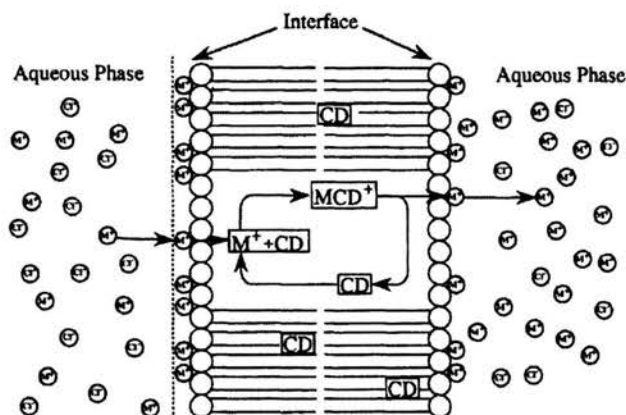


FIGURE 11. Schematic diagram showing the carrier mechanism of ion transport across lipid bilayer.  $M^+$  is a cation, CD – molecule of carrier; taken from [16].

In the presented study transport of different cations by cyclodextrin derivatives was investigated. Cyclodextrins are typical carriers because in their structure they possess a hydrophilic pocket in which the guest molecules (ions) can be hidden during the passage across the hydrophobic part of membrane. Cyclodextrin derivatives studied were added to the solution used for the formation of BLMs. Conductance (reciprocal of resistance) of BLMs was measured as a ratio of recorded current to the applied voltage. The plot

of conductivities of BLMs containing different cyclodextrin derivatives as a function of the ion radii is presented in Fig. 12.

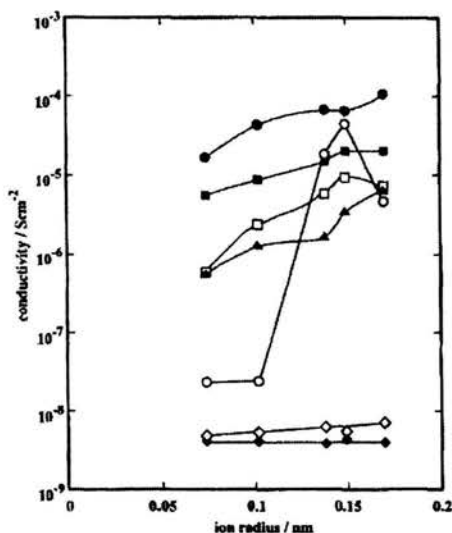


FIGURE 12. Conductivities of BLMs in the absence ( $\diamond$ ) and presence of  $10^{-3}$  M valinomycin ( $\circ$ ) and cyclodextrin derivatives ( $\bullet$ ,  $\blacksquare$ ,  $\square$ ,  $\triangle$ ,  $\blacklozenge$ ) as a function of the cation radius; taken from [16].

Comparing the results obtained for valinomycin and studied cyclodextrins the authors concluded that unlike valinomycin (preferring  $K^+$  ions – 0.138 nm) cyclodextrins do not show special preference to any of the studied ions ( $Li^+$ ,  $Na^+$ ,  $K^+$ ,  $Rb^+$ ,  $Cs^+$ ). By preparing the BLMs containing different concentrations of cyclodextrins it was also shown that conductivity of membranes is proportional to the number of cyclodextrin molecules. This supports the carrier model proposed for the mechanism of ion transport carried out by these molecules.

### 2.3. Liposomes

Multi- or unilamellar liposomes (or vesicles) can be obtained using different techniques, which vary from simple shaking up to extrusion through the porous membrane. Among the different experimental models of liposomes, consider the most closely resembling membranes of living cells. First of all, lipid bilayer in this case is a barrier dividing the space into two well defined compartments: inner (corresponding to the cytoplasm of the cell) and outer (corresponding to the cells' surrounding). On the other hand, the barrier

properties of liposome membrane could be easily set or modulated by proper choice of lipids used for the production of liposomes. Using different combinations of lipids it is possible to mimic in this way the properties of different cell membranes. Special techniques of production enable also to obtain the liposomes possessing asymmetric membranes – differing in the composition of outer and inner leaflets. Another advantage of liposomal techniques is that it is possible to produce liposomes (or vesicles) of the desired size. Such possibility is of extreme importance in studies on the role of membrane curvature in different processes and also when optical control of membrane domains formation is performed.

Presumably the most simple and classic application of liposomes is using them as a model membranes in the studies on the bilayer permeability. As an example of such a studies the influence of inhalation anaesthetics on the efflux of carboxyfluorescein from liposomes [6] is described below.

The molecular mechanism of anaesthetics action is still unclear and two general concepts are discussed. First of them regards neuron membrane proteins as a primary target for anaesthetics, the second one focuses on the non-specific interactions of drug molecules with the lipid matrix of membrane. Reported here studies are based on the second concept and were performed partially to investigate the influence of chosen inhalation anaesthetics on the passive permeability of liposomal membranes. Liposome permeability was measured using carboxyfluorescein assay. CF is a fluorescent dye which at high enough concentrations self-quenches its fluorescence. The liposomes for these studies were prepared from the mixture of egg yolk PC with 0, 20 or 40 mol% cholesterol in a buffer containing additionally 150 mM CF. Fluorescent dye not trapped inside liposomes was removed chromatographically using Sephadex G50 column at 4° C. During the experiment different amounts of anaesthetics (10, 20, 30, 40 and 50 mol%) were added to liposome suspension and carboxyfluorescein leakage from liposomes was measured using spectrofluorimeter. At the end of experiment liposomes were solubilised (destroyed) by detergent Triton X-100. This step was necessary to estimate the total amount of CF encapsulated inside liposomes. Percent of CF leakage from liposomes was calculated using the following formula:

$$CF_{\text{leak}} = 100(F_b - F_a)/(F_t - F_a), \quad (2.1)$$

where  $F_b$  is the fluorescence intensity before addition of anaesthetic,  $F_a$  - fluorescence intensity after the addition of anaesthetic,  $F_t$  - fluorescence intensity after solubilization by Triton X-100. Due to CF self-quenching most of the fluorescence measured in such an experiment comes from the CF molecules that are in external solution and is proportional to the permeability of liposome membrane. It was found that all studied anaesthetics: halothane,



chloroform, diethyl ether, enflurane and n-pentane increase liposome permeability to CF in a concentration-dependent manner. Halothane, chloroform and diethyl ether were the most effective independently of the composition of liposome bilayers. For all anaesthetics studied their effects exerted on membrane permeability were dependent on the amount of cholesterol – the higher was concentration of sterol the less membranes were perturbed by anaesthetics.

More sophisticated applications of liposomes include experiments performed on reconstituted proteins. Process of protein reconstitution is used to separate protein molecule from its natural surrounding and to put it into well defined membrane. Reconstitution is performed to reach one of the following goals:

- (i) to study single, isolated type of protein instead of many (as it usually happens in natural membranes), or
- (ii) to decide about the composition of membrane and thus fully control the situation in which protein is active/inactive. The studies on the importance of cholesterol in maintenance of P-glycoprotein activity in reconstituted systems [22] will be used here as an example of application of this method.

P-glycoprotein is overexpressed in membranes of many multidrug resistant cancer cells and the outward, active transport of anticancer drugs carried out by this protein is one of the reasons of chemotherapy failure [7]. Several studies has proved that transport activity of P-gp depends upon the physical state of membrane as well as on its lipid composition (for a review see [12]). On the other hand it was found that P-gp alters the fluidity and organization of membranes of cells in which is overexpressed. The described below work was devoted to elucidate the role of cholesterol as a factor influencing the P-gp activity on one hand and to determine the extent of membrane perturbation induced by this protein.

In the first step of reconstitution procedure P-glycoprotein was extracted from the cellular membranes and purified to obtain more than 60% of protein in the preparation. Liposomes were produced using a mixture of PC and PE (9 : 1 w/w) with the addition of different amounts of cholesterol: 5, 10, 20 and 30% (w/w). Reconstitution of P-gp was achieved by the removal of detergent from the protein/liposome/detergent mixture. The sucrose gradient centrifugation was used finally to determine the efficiency of reconstitution procedure.

Liposomes loaded with P-gp were then used to study the influence of P glycoprotein, cholesterol content and temperature on the fluidity of membranes containing reconstituted protein. Fluidity of liposome membranes was

assessed by means of TMA-DPH fluorescence polarization measurements. TMA-DPH is a fluorescent dye which incorporates into the lipid bilayers. In rigid surrounding the dye molecules have restricted motional freedom and the light emitted by them is polarized parallel to the polarization of excitation beam. In more fluid membranes TMA-DPH molecules could rotate or translate more freely between the excitation and emission moments and polarization of emitted light parallel to the polarization of excitation beam decreases. The degree of polarization is a parameter calculated using the intensities of light polarized parallel ( $I_{||}$ ) and perpendicular ( $I_{\perp}$ ) to the polarization of the incident, excitation beam:

$$P = \frac{I_{||} - I_{\perp}}{I_{||} + I_{\perp}}. \quad (2.2)$$

The degree of TMA-DPH fluorescence polarization in liposomes made of pure lipids and proteoliposomes was compared for samples containing different cholesterol content (0, 5, 10, 20 and 30% w/w). It was found that increasing cholesterol amounts rises the TMA-DPH polarization degree and reduce the fluidity of both types of liposomes. Presence of P-gp in membranes resulted, however, in the decrease of TMA-DPH polarization degree in comparison to the pure lipid liposomes. This means that P-gp after incorporation into the membrane increases its fluidity but this increase should be reversed by addition of the appropriate amount of cholesterol. The dependence of liposome and proteoliposome fluidity upon the temperature was also studied and for rising temperature a decrease of TMA-DPH polarization degree was found. In temperature studies presence of P-gp in membranes produced an effect similar to investigation on the role of cholesterol.

Apart from the fluidity measurements also the proteoliposome (i.e. liposomes containing reconstituted P-gp) membranes permeability for dithionite, and P-gp ATP-ase activity were determined. It was found that the presence of cholesterol in proteoliposome membranes enhances the ATP-ase activity of P-gp in a cholesterol concentration-dependent manner.

### 3. Theoretical models

Theoretical models intend to predict the macroscopic properties of the systems of interest (like lipid bilayers, proteins, etc.) using different mathematical and/or computational methods. Most of such models use some basic parameters describing the initial micro- or macroscopic state of the system as a starting point. The initial parameters of any model are generally derived from the experimental data or describe some real situation (like composition of a mixture). Since the biological systems are far too complicated for

direct determination of the most of indispensable data, the input for theoretical models very often is based on the quantities describing experimental models. To give the simplest example: the length of hydrocarbon chains of biological membranes varies so much that for theoretical models usually one length (corresponding to a certain experimental model, e.g. lipid molecule) is usually taken.

Models used for theoretical description of (quasi) biological systems differ strongly in their complexity. Some models of binary lipid mixtures are able to describe properly the phase behaviour of such systems using a set of simple mathematical equations that can be solved using a pencil and a sheet of paper. On the other hand, molecular dynamics or Monte Carlo simulations use sophisticated mathematics and computational methods. They also need top computers to predict the behaviour of single protein molecule in lipid bilayer (total of 19 000 atoms all together) during the time interval as long as 500 ns.

To give a rough overview of the theoretical models used in biophysics I will describe below the following modelling approaches. First, the method for calculation of parameters describing mechanical properties of lipid bilayer from the thermodynamic data will be described. Further, the example mechanical model of the cell (liposome) membrane shape changes will be shortly described. Subsequently I will give a short description of basic ideas underlying the molecular dynamics and Monte Carlo simulations and usage of those methods in lipid bilayer and protein modelling will be presented.

### 3.1. Modelling of lipid bilayer properties

An example of work showing that using appropriate model one can calculate the values of many parameters describing the considered system is the contribution by Heimburg [10]. In his work he focused on the coupling between the thermodynamic and mechanical properties of lipid. As it is assumed for molecular dynamics or Monte Carlo models (see Sec. 3.3) he defines the parameters of a certain thermodynamic system as average values of experimental observables:

$$\langle X \rangle = \frac{1}{Q} \sum_i X_i \Omega_i \exp \left\{ -\frac{H_i}{RT} \right\}, \quad (3.1)$$

where  $X_i$  is the calculated value (in this work energy, volume or area of lipid matrix) and  $Q$  is a partition function given by:

$$Q = \sum_i \Omega_i \exp \left\{ -\frac{H_i}{RT} \right\}. \quad (3.2)$$

In both above equations  $\Omega_i$  is a degeneracy of states with identical Hamiltonian energies. According to the thermodynamic definitions the heat capacity at constant pressure ( $c_p$ ), isothermal volume and area compressibilities ( $\kappa_T^{\text{vol}}$  and  $\kappa_T^{\text{area}}$ , respectively) are the derivatives of the enthalpy, volume and area of lipid bilayer:

$$\begin{aligned} c_p &= \left. \frac{d\langle H \rangle}{dT} \right|_p = \frac{\langle H^2 \rangle - \langle H \rangle^2}{RT^2}, \quad \kappa_T^{\text{vol}} = -\frac{1}{\langle V \rangle} \left. \frac{d\langle V \rangle}{dp} \right|_T = \frac{\langle V^2 \rangle - \langle V \rangle^2}{\langle V \rangle RT}, \\ \kappa_T^{\text{area}} &= -\frac{1}{\langle A \rangle} \left. \frac{d\langle A \rangle}{d\Pi} \right|_T = \frac{\langle A^2 \rangle - \langle A \rangle^2}{\langle A \rangle RT}. \end{aligned} \quad (3.3)$$

As can be seen from Eq. (3.3) the heat capacity, volume and area compressibilities correspond to the fluctuations of the enthalpy, volume and area of the bilayer, respectively. As it was described in Sec. 1.1 during the phase change of lipid systems we observe drastic changes of almost all parameters describing the bilayers. Also the heat capacity, volume and area compressibilities alter and the changes of those parameters will be denoted further as excess values (during the transition) –  $\Delta c_p$ ,  $\Delta \kappa_t^{\text{vol}}$  and  $\Delta \kappa_t^{\text{area}}$ , respectively. For lipid mixtures it was proved that the average volume change during the phase transition is proportional to the average enthalpy change of this transition:

$$\langle \Delta V(T) \rangle = \gamma_{\text{vol}} \langle \Delta H(T) \rangle, \quad (3.4)$$

where  $\gamma_{\text{vol}}$  is the proportionality constant. By differentiating Eq. (3.4) with respect to the temperature we obtain:

$$\frac{d\langle \Delta V \rangle}{dT} = \gamma_{\text{vol}} \frac{d\langle \Delta H \rangle}{dT} = \gamma_{\text{vol}} \Delta c_p. \quad (3.5)$$

As a consequence of Eqs. (3.3) and (3.5) the excess bilayer compressibilities can be expressed as a function of the excess heat capacity  $\Delta c_p$ :

$$\Delta \kappa_T^{\text{vol}} = \frac{\gamma_{\text{vol}}^2 T}{\langle V \rangle} \Delta c_p, \quad \Delta \kappa_T^{\text{area}} = \frac{\gamma_{\text{area}}^2 T}{\langle A \rangle} \Delta c_p. \quad (3.6)$$

If a lipid bilayer is exposed to mechanical stress it undergoes a deformation which is dependent upon the bending modulus  $K_{\text{bend}}$ . Instead of bending modulus we can use bending elasticity, defined as a reciprocal of modulus:  $\kappa_{\text{bend}} = 1/K_{\text{bend}}$ . For a lipid bilayer of thickness  $D$ ,  $\kappa_{\text{bend}}$  can be calculated, from the area compressibility as:

$$\kappa_{\text{bend}} = \frac{16\kappa_T^{\text{area}}}{D^2}. \quad (3.7)$$

When the lipid bilayer is passing through the phase transition the bending elasticity changes and (like for previously defined excess parameters) we can relate excess bending elasticity to the excess heat capacity:

$$\Delta\kappa_{\text{bend}} = \frac{16\gamma_{\text{area}}^2 T}{D^2 A} \Delta C_p. \quad (3.8)$$

Since this section is concerned with theoretical models I will only add that in experimental part of Heimburg's work an excellent proof for the correctness of Eq. (3.4) is presented. It shows that the heat capacity and volume change profiles during the main DMPC transition superimpose, even in minute details, see Fig. 13. The relation between the thermotropic behaviour of DPPC bilayers and their mechanical properties was also shown in this work.

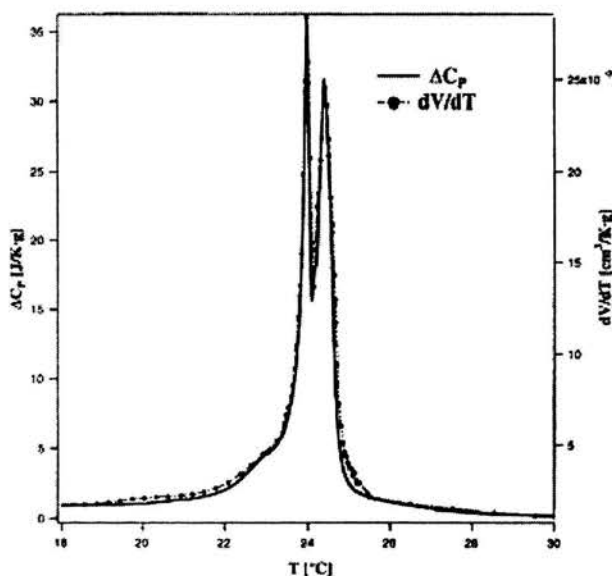


FIGURE 13. Heat capacity profile of the main transition of extruded DMPC with the temperature dependence of the specific volume. The volume expansion coefficient is nearly superimposable with the  $\Delta C_p$  profile (after [10]).

### 3.2. Cell shape modelling

As described in Sec. 1.3 erythrocytes change shape when their membranes bind drug molecules. Similar shape changes can be also observed for liposomes with the addition of small amounts of detergent. Since a variety of shapes is usually possible for such systems a theoretical model has been proposed to

give an explanation for the experimentally observed effects [28]. The basic rationale for this model is that any membrane shape must correspond to the minimum of the membrane elastic energy. In general elastic energy consist of stretching, shear and bending components. Since membrane area is practically constant the stretching component might be neglected, also shear energy has minimal importance due to the relatively big fluidity of membranes. Thus only bending energy should be considered as a factor determining the shape of membrane.

Assuming that model membrane is characterised by elastic constant  $\kappa$  and two principal curvatures  $C_1$  and  $C_2$  for a bending elastic energy of such membrane we obtain:

$$W_b = \frac{1}{2}\kappa \int (C_1 + C_2)^2 dA^*, \quad (3.9)$$

where the integration is made over the whole area of the bilayer  $A^*$ . Since in this model the area difference between the outer and inner membrane layers ( $\Delta A$ ) is also considered the area  $A^*$  corresponds to the surface located right in the middle of membrane. The elastic bending energy should be minimized at fixed values of cell volume ( $V$ ), area of membrane ( $A$ ) and difference of the inner and outer membrane layer areas ( $\Delta A$ ). The minimization procedure was performed using the Lagrange multiplier method. For the convenience of calculations instead of normal variables the relative dimensionless new variables were introduced. New unit of length is defined as the radius of sphere and the area of the considered membrane:  $R_s = (A/4\pi)^{1/2}$ . The new variables are introduced using this unit and are defined as follows:

$$\begin{aligned} c_1 &= R_s C_1; & c_2 &= R_s C_2, \\ v &= V/V_s; & V_s &= 4\pi R_s^3/3, \\ \Delta a &= \Delta A/\Delta A_s; & \Delta A_s &= 8\pi\delta R_s, \end{aligned} \quad (3.10)$$

while the relative area  $a = 1$ . Using those new variables and performing minimization of the function given by Eq. (3.9) the function describing the shapes is obtained. This function was first analyzed with the respect to the limiting shapes which could be obtained for extreme values of relative volumes ( $v_e$ ). In Fig. 14 relative volumes are plotted as a function of relative area difference between the inner and outer membrane layers ( $\Delta a$ ). The shapes that correspond to certain points of the  $v_e(\Delta a)$  diagram are also presented. The presence of shapes (2, 3, 4) consisting of one big sphere and one (or more) small spheres is an interesting result shown in this figure. Such a membrane behaviour could be related to the of erythrocyte vesiculation – phenomenon

occurring when erythrocytes are exposed to the action of certain amphiphilic surfactants or drugs [9].

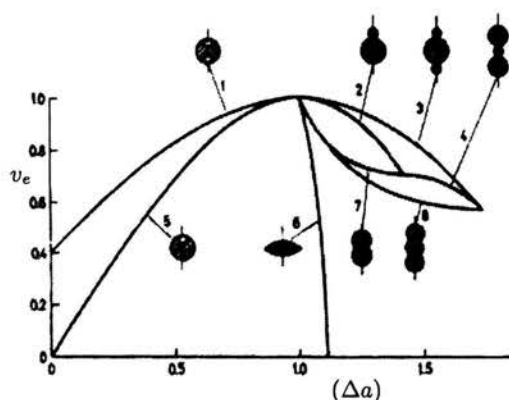


FIGURE 14. The limiting shapes corresponding to the extreme relative volumes ( $v_e$ ) as a function of the relative leaflet area difference ( $\Delta a$ ); after [28]. For details see text.

The shapes presented in Fig. 14 represent a whole family of possibilities. Since at least some of them seem to be rather unrealistic it is reasonable to study only that class of shapes which can be derived from the  $v$  and  $\Delta$  the values corresponding to the situation found in erythrocytes. Two classes were studied in this way: discoidal and cup-like shapes. The shapes were obtained for relative volume 0.6 and varying relative area difference  $\Delta a$ . This simulation corresponds to the experimental situation in which a cell with constant volume and membrane area interacts with drug or detergent that is changing the area of one of the membrane leaflets. In Fig. 15 the examples of shapes belonging to two discussed classes are presented together with values of corresponding  $\Delta a$  and membrane elastic bending energy.

As presented in Fig. 15 the transformation of erythrocyte membrane from normal (discoidal) shape to the stomatocyte is related with decrease of relative area difference ( $\Delta a$ ). This result is in agreement with the bilayer coupling hypothesis – decrease of  $\Delta a$  corresponds to the expansion of inner leaflet or to the decrease of outer membrane layer area.

### 3.3. Molecular dynamics simulations vs. Monte Carlo methods

Molecular dynamics and Monte Carlo simulations are presumably the best tools for theoretical studies of behaviour of such biological systems as lipid bilayers, proteins or nucleic acids. Using these methods it is possible to follow

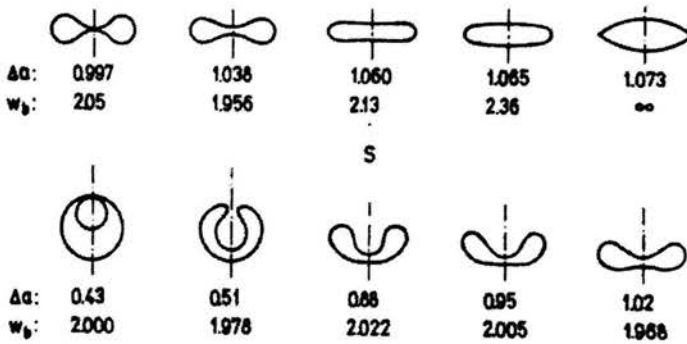


FIGURE 15. Characteristic examples of symmetrical discoidal shapes and asymmetrical shapes at relative volume  $v = 0.6$ . The corresponding leaflet area differences and relative membrane bending energies are given in the figure; after [28].

the behaviour of systems containing several thousands of atoms, but due to contemporary computer capabilities the time scale of simulations is rather short. The main difference between these two methods is that molecular dynamics is a fully deterministic method while the Monte Carlo method uses probabilistic approach.

The molecular dynamics method calculates the time dependent behaviour of a given molecular system. As a starting point for simulation the detailed microscopic description of the system under investigation must be given. It means that positions and momenta of all atoms present in the system must be prescribed. Both atomic positions and momenta can be considered as coordinates in multidimensional space (phase space) which for system containing  $N$  atoms has  $6N$  dimensions. A collection of points in phase space (each corresponding to certain system state) satisfying the conditions of particular thermodynamic state is called an ensemble. Once the ensemble is described the macroscopic parameters of the system can be defined as ensemble averages of the experimental observables. The ensemble averages are calculated using the statistical mechanics according to the general formula:

$$\langle A \rangle_{\text{ens}} = \iint A(p^N, r^N) \rho(p^N, r^N) dp^N dr^N, \quad (3.11)$$

where  $p$  and  $r$  are momenta and positions of the system components, respectively,  $A(p^N, r^N)$  is an experimental observable. The probability density of the ensemble is given by

$$\rho(p^N, r^N) = \frac{1}{Q} \exp[-H(p^N, r^N)/k_B T], \quad (3.12)$$



where  $H$  is the Hamiltonian,  $T$  – temperature,  $k_B$  – Boltzmann's constant and  $Q$  is the partition function defined by:

$$Q = \iint \exp[-H(p^N, r^N)/k_B T] dp^N dr^N. \quad (3.13)$$

Calculation of integral in Eq. (3.11) is extremely difficult and therefore (according to ergodic theorem) ensemble average  $A_{\text{ens}}$  is replaced by time average  $A_t$  expressed by:

$$\langle A \rangle_{\text{ens}} = \langle A \rangle_t = \lim_{\tau \rightarrow \infty} \frac{1}{\tau} \int_{t=0}^{\tau} A(p^N(t), r^N(t)) dt \approx \frac{1}{M} \sum_{t=1}^M A(p^N, r^N), \quad (3.14)$$

where  $t$  is the simulation time and  $M$  is the number of time steps in the simulation.

The basic assumption for ergodic theorem is that when system is evolving during infinite time it will pass through all possible conformations. Thus performing a real simulations (in limited time) one must be sure that a representative number of conformations has been generated.

To predict the trajectories of all atoms in the phase space it is necessary to know also the forces acting on each atom, apart from the initial atoms positions and momenta. As a consequence of the Newton's Second Law forces can be expressed in terms of energy gradients and therefore trajectories are calculated from the potential energy functions.

$$F = am = -\frac{dE}{dr}. \quad (3.15)$$

The acceleration  $a$  calculated from the Eq. (3.15) together with the initial values of positions ( $r_0$ ) and velocities ( $v_0$ , derived from momentum  $p_0$  as  $v_0 = p_0/m$ ) are used to determine the positions and velocities of atoms as functions of time:

$$\begin{aligned} r &= at^2 + v_0 t + r_0, \\ v &= at + v_0. \end{aligned} \quad (3.16)$$

Since potential energy of the system is a function of atomic positions ( $3N$  variables) analytical integration of Eq. (3.15) is impossible and calculations of  $r$  and  $v$  must be performed numerically. To perform such calculations several algorithms are used, all of them assume that positions, velocities and accelerations are expressed by the Taylor series expansion.

Another problem related to the energy function is that for a molecular system the best way to express this function is to calculate it using quantum

mechanics. Quantum mechanical approach is, however, computationally demanding and to reduce the amount of calculations empirical or semi-empirical potential energy functions are used. While using the approximated energy function one encounters some limitations, which differ depending on the type of approximation applied. Among the most commonly used force fields are the AMBER, CHARMM and GROMOS potential energy functions. All the approximations use the parameters obtained experimentally, are calibrated to experimental results and available results of quantum mechanical calculations. The main limitation of empirical approximations of force fields is that no drastic changes in electronic structure of the system are allowed. It means that during the simulation no chemical bonds could be generated or broken, for example.

Monte Carlo methods are numerical methods in which statistical simulation is used to obtain the values of parameters describing the studied system. To give a very simple example of such statistical simulation let me present the stochastic method of calculation of  $\pi$ . This method is well suited for the poor darts players since is based on random hits to the dart target. Instead of full target we will consider a quarter of it, see Fig. 16. Throwing randomly on this target we easily come to conclusion that probability ( $P$ ) of reaching the black area is proportional to the ratio of its area ( $A_{\text{black}} = 0.25\pi r^2$ ) and area of a square ( $A_{\text{sq}} = r^2$ ) representing whole dart target:

$$P = \frac{A_{\text{black}}}{A_{\text{sq}}} = \frac{0.25\pi r^2}{r^2} = 0.25\pi. \quad (3.17)$$

Thus  $\pi = 4P$  and after 1000 shots we obtain a very rough estimation – 3.60!! The accuracy of estimation improves, however, when we increase the number of shots, after 10000 shots we obtain much better value of 3.51.

System properties calculated by Monte Carlo methods are obtained like in the molecular dynamics approach – as averages of experimental observables (see Eqs. 3.11 and 3.17). The main difference between these two methods is the way in which certain method switches between subsequent (or different) system states. In MD method new positions and velocities are calculated as functions of time but in the MC simulations system states are randomly chosen from the set of all possible configurations.

### 3.4. Computerised modelling of proteins and lipid bilayers

As the first example of a membrane molecular model the theoretical study of the dynamic properties of hydrated dimyristoylIPC bilayers [20] will be presented. Since many years different properties of lipid bilayers have been studied and much is known on this subject. Nevertheless, theoretical studies

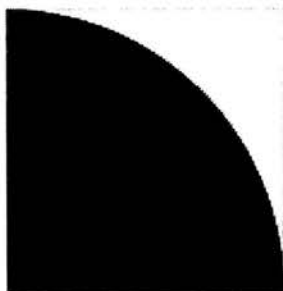


FIGURE 16.  $\frac{1}{4}$  of the darts target should be used for  $\pi$  approximation.

are performed to compare the values of different membrane parameters obtained as experimental results and theoretical predictions. A positive result of such comparison confirms that right calculation methods has been chosen and enables to use properly constructed model to study problems that has not been solved yet experimentally.

In the paper by Moore et al. [20] a simulation was performed for the system consisting of 64 lipid molecules and 1792 water molecules. The number of water molecules was set to allow a proper hydration of lipid bilayer. The system was built in consecutive steps: starting from 8 lipid molecules the number of lipids in bilayer was doubled three times and after each step the structure was allowed to relax for a few picoseconds. For each lipid molecule 28 waters were added. Finally 500 ps simulation was performed at constant volume and temperature (333 K) of the system. Apart from some other information obtained from simulation the order parameter of carbon atoms along the acyl lipid chains was calculated. Order parameter  $S_{CD}$  was originally defined as a parameter calculated using the NMR data (obtained for deuterated lipid acyl chains) and gives a measure of average methylene group orientation with respect to the bilayer normal. The  $S_{CD}$  is defined as:

$$S_{CD} = \left\langle \frac{1}{2}(3 \cos^2(\beta) - 1) \right\rangle, \quad (3.18)$$

where  $b$  is the angle between a vector normal to the plane formed by carbon and deuterium (hydrogen in simulation) atoms and a vector normal to the bilayer. Information given by  $S_{CD}$  corresponds to polarization degree obtained in fluorescence measurements. Order parameter describes the rotational freedom of acyl chains; it decreases when rotation of methylene group increases and the acyl chain becomes more fluid.

Using MD data the order parameters were calculated for carbon atoms along both sn-1 and sn-2 acyl chains. In Fig. 17 the  $S_{CD}$  values obtained

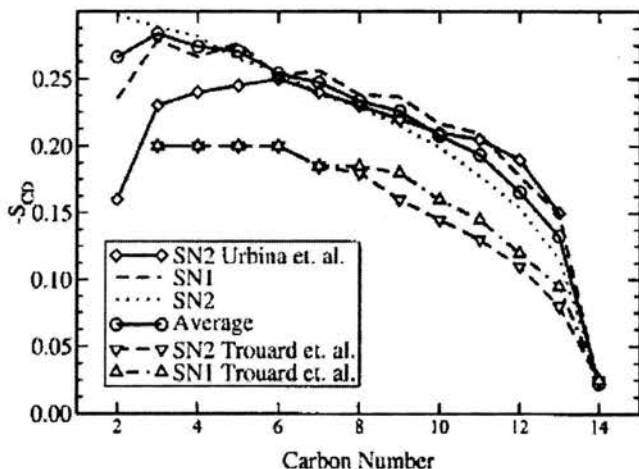


FIGURE 17. Order parameter profiles as function of carbon atom position along the sn-1 (---) and sn-2 (···) chain. Theoretical and experimental data obtained by other authors are plotted for comparison; after [20].

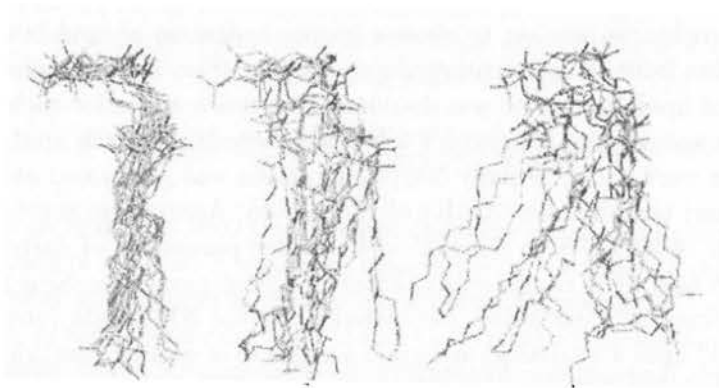


FIGURE 18. Snapshots of set of lipid molecules structure for different time intervals of simulation (left to right 100 ps, 1 ns, 10 ns); after [20].

from simulation together with data calculated for experimental results by two different authors (the reference of these authors is not given here) are plotted as a function of carbon atom position in the chain. A nice agreement between theoretical and experimental data was found – starting from the polar head-group region first 5 – 7 carbons in acyl chains are much more ordered than carbons located closer to the bilayer center. Such fluidity gradient was found in lipid bilayers also by other experimental methods.

To illustrate the dynamics of lipids the superimposed motion of single lipid molecule observed in different time scales is presented in Fig. 18. On 100 ps time scale the intramolecular vibrations and few torsional *trans-gauche* bond flips could be observed. On 1 ns time scale the increased amplitude of motion is seen. Lipid molecule start to translate and rotate, much more torsional *trans-gauche* flips appear in the acyl chain region. The head group region of lipid molecule remains at almost original position and is oriented in roughly the same direction. On 10 ns time scale the lateral diffusion of lipid molecule can be seen, hydrocarbon chains region shows a large amplitude of motion.

In another simulation the influence of cholesterol on the properties of dimyristoylPC bilayers [23] was investigated using molecular dynamics simulation. In this case the studied system consisted of 56 molecules of phospholipid, 16 molecules of cholesterol (what corresponds to the 22 mol% of cholesterol) and 1622 water molecules to provide hydration of bilayer.

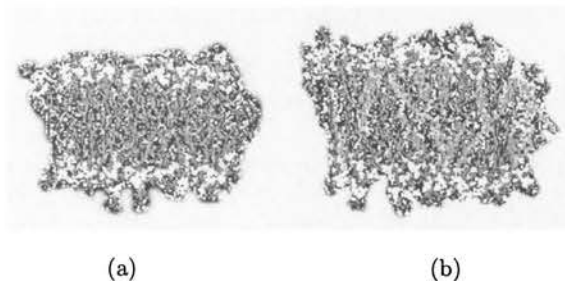


FIGURE 19. Dimyristoylphosphatidylcholine bilayer after the 12 ns of equilibration (a) and dimyristoylPC-cholesterol mixture after 10 ns of simulation (b); from [23].

In Fig. 19 the structures obtained for dimyristoylPC (after 12 ns of simulation) and dimyristoylPC-cholesterol mixed (after 10 ns simulation) bilayers are presented. As it can be judged from this figure (and what is confirmed also by certain simulation data) cholesterol increases the thickness of lipid bilayer for about 2 Å. Cholesterol molecules are randomly dispersed throughout the studied system but their polar parts are always anchored close to the polar/apolar interface of each lipid leaflets.

Data obtained from simulation were used to characterise the factors determining fluidity (or rather motional freedom) of lipid acyl chains. In Fig. 20 the probabilities of *gauche* conformations along sn-1 and sn-2 lipid chains are plotted as a function of a position in the chain and plots are prepared for dimyristoylPC as well as for dimyristoylPC - cholesterol mixtures. The presence of cholesterol slightly decreases probability of *gauche* conformation in sn-1 chains but shows practically no effect in sn-2 lipid chains.

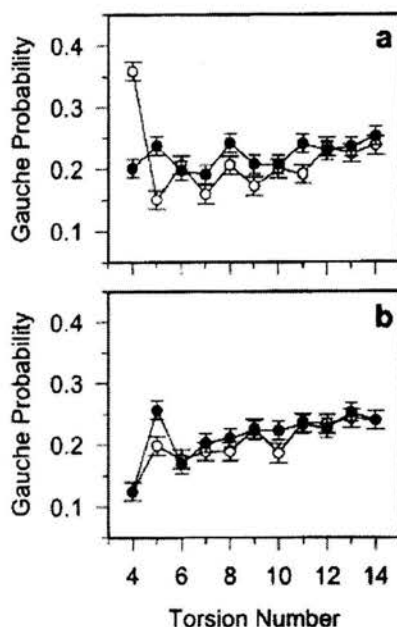


FIGURE 20. Probabilities of gauche conformation in sn-1 (a) and sn-2 (b) chains of pure DMPC (●) and DMPC-cholesterol mixture bilayers (○); after [23].

Similarly to work of Moore et al. [20], also in this paper the order parameter  $S_{\text{mol}}$  of acyl chain carbons was calculated. The  $S_{\text{mol}}$  values are plotted in Fig. 21 as a function of carbon atom location along the chain for both pure dimyristoylPC and dimyristoylPC-cholesterol bilayers. As can be seen modification of bilayer properties by the addition of 22 mol% of cholesterol results in the increase of molecular order along the whole length of lipid acyl chains. Presence of cholesterol, however, does not influence the effect of chain fluidity gradient, which is visible for pure lipid as well as for lipid-cholesterol mixtures.

Molecules of many drugs are amphiphilic or hydrophobic. Such a molecules intercalate into lipid bilayers and change the biophysical properties of membrane lipid phase. In many cases the alteration of lipid matrix properties is at least partially related to the therapeutic effects of certain drug. For this reason many types of studies – both experimental and theoretical, focus on the problem of drug-membrane interactions. As an example of a molecular dynamic simulation of the drug-membrane interactions, the model consisting of dihydropyridine molecules intercalated in DMPC bilayer will be described [1]. Dihydropyridines are known as calcium channel antagonists or

agonists, i.e. compounds that modulate the properties of the channel. Due to their hydrophobicity dihydropyridines could penetrate the hydrophobic core of membranes, what determines the pharmacokinetics of those drugs. For this reason studies on dihydropyridine-lipid interactions can deliver further information needed for the design of new, better drugs.

In the first step of modelling procedure the initial conformation of lipid

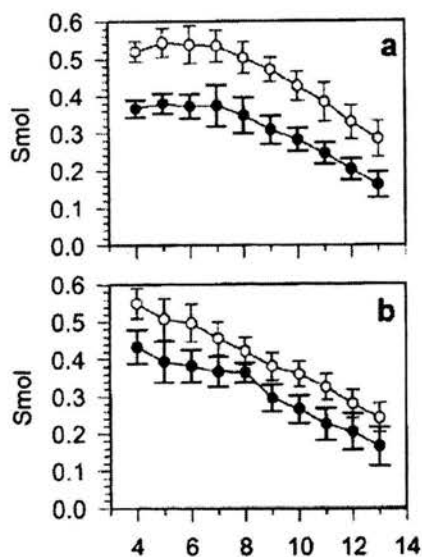


FIGURE 21. Order parameter profiles ( $S_{mol}$ ) calculated for sn-1 (a) and sn-2 (b) chains of pure dimyristoylPC (●) and dimyristoylPC-cholesterol mixture (○) bilayers; after [23].

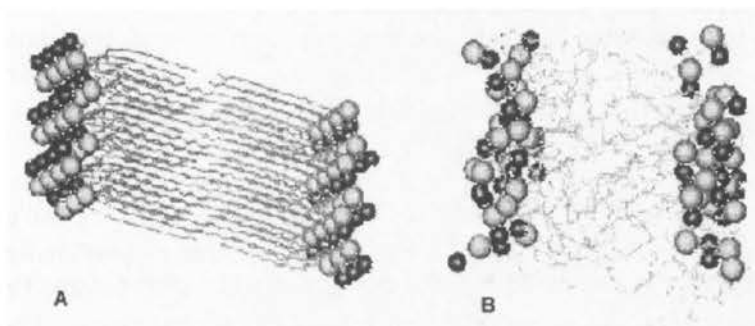


FIGURE 22. Modelling of DMPC bilayer. A – lipid bilayer constructed with 42 lipid molecules (21 in each layer). B – the same bilayer after the 550 ps molecular dynamics simulation; after [1].

bilayer containing 42 dimyristoylphosphatidylcholine (DMPC) molecules (21 per one membrane layer) was constructed using the crystallographic data. This initial bilayer structure is shown in Fig. 22A. The molecular dynamics simulation was performed CHARMM, one of the most commonly used force fields approximations. Before the simulation the energy of the system was minimized. The calculations were made in few steps: first the system was heated to 325 K (for 10 ps) and then equilibrated for next 40 ps. For the next 550 ps model was allowed to evolve freely at constant temperature, which was controlled during the whole time of this simulation step. In Fig. 22B the final configuration of the model is shown. Since the temperature of the system was well above the main transition temperature of DMPC (which is 297 K) the bilayer is in liquid-crystalline state and lipid hydrocarbon chains are melted – this is clearly seen in Fig. 22B. The correctness of the obtained structure was checked by the comparison of lipid bilayer thickness of the model (measured as phosphorus-phosphorus distance) and the X-ray diffraction data. General agreement between those data was found; however, model thickness was slightly smaller, presumably due to fact that water molecules were ignored in simulation.

In the last part of simulation the molecules of drugs (nifedipine and lacidipine) were included into the model. Primary location of the drugs was chosen according to the X-ray diffraction data. After the minimization of the energy of the system simulation has been performed in steps similar to those used in pure *DMPC* simulation. After heating (10 ps) and equilibration (100 ps) the system was allowed to evolve freely during the 600 ps run. In Fig. 23A the structure of bilayer with drug molecule after 350 ps of simulation is presented, while in Fig. 23B the drug molecule and only six closest to it lipid molecules are depicted.

The effect exerted by DPH molecules on the lipid hydrocarbon chains was analysed by the calculation of the fraction of chain trans conformations. Since this fraction has not changed after addition of drugs to the bilayer structure it was concluded that packing of lipid chains was not seriously altered by the presence of dihydropyridine molecules.

Monte Carlo simulation was used for the modelling of behaviour of  $\alpha$ -helical peptides in lipid bilayers [27]. The parameters describing the studied systems were chosen to enable the analysis of the role of peptide-lipid hydrophobic matching (see Sec. 1.2) in the aggregation of peptides. Peptides are assumed to be identical, rigid objects of cylindrical shape. They can be hydrophobic or partially hydrophilic. Each peptide occupied seven sites in triangular bilayer lattice. The bilayer model used in this study was constructed according to the Pink model [21] in which bilayer is formed from two independent monolayers, each represented by triangular lattice. For each



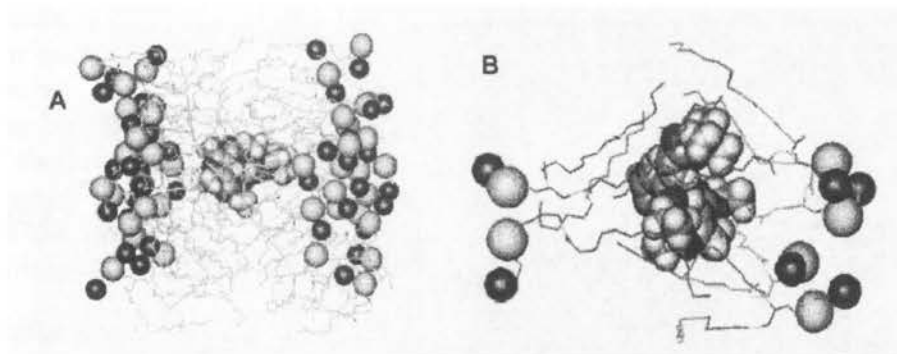


FIGURE 23. Interaction of nifedipine molecule with DMPC lipid bilayer. A - configuration of the system after 350 ps simulation. B - the drug molecule shown together with six closest lipid molecules; after [1].

chain ten different conformational states are possible, each of which is characterized by an internal energy ( $E_m$ ), hydrocarbon chain length ( $l_m$ ) and degeneracy ( $D_m$ ) accounting for the number chain conformations described by the same energy. The ten state model was derived from experimentally observed trans-gauche isomerization of lipid chains. The state  $m = 1$  is the non degenerated gel-like state while state  $m = 10$  corresponds to the highly degenerated fluid state of lipid hydrocarbon chains.

The Hamiltonian functions used within this model described lipid-lipid as well as lipid-peptide and peptide-peptide interactions. The Hamiltonian for lipid-lipid interactions is expressed as:

$$H_{L-L} = \sum_i \sum_m (E_m + \Pi A_m) L_{m,i} - \frac{J_0}{2} \sum_{\langle i,j \rangle} \sum_{m,n} I(d_m, d_n) L_{m,i} L_{n,j}, \quad (3.19)$$

where  $\Pi$  is a lateral pressure,  $J_0$  is the strength of van der Waals forces between neighbouring chains,  $I(d_m, d_n)$  is an interaction matrix which involves both distance and shape dependence,  $L_{m,i}$  are state occupation variables. The Hamiltonian for lipid-peptide interactions in the hydrophobic regions of peptides is written as:

$$\begin{aligned}
H_{L-P} &= \Pi \frac{A_p}{7} \sum_j L_j - \frac{v}{2} \sum_{i,j} \sum_m \min(d_{m,i}, d_p) L_{m,i} L_j \\
&\quad + \frac{2\gamma}{2} \sum_{i,j} \sum_m |d_{m,i} - d_p| L_{m,i} L_j, \quad \text{if } d_p < d_{m,i}, \\
H_{L-P} &= \Pi \frac{A_p}{7} \sum_j L_j - \frac{v}{2} \sum_{i,j} \sum_m \min(d_{m,i}, d_p) L_{m,i} L_j \\
&\quad + \frac{\gamma}{2} \sum_{i,j} \sum_m |d_{m,i} - d_p| L_{m,i} L_j, \quad \text{if } d_p > d_{m,i},
\end{aligned} \tag{3.20}$$

where  $L_i$  are peptide-site occupation variables. For hydrophilic regions of peptides Hamiltonian function is similar to that of Eq. (3.20), the only difference is that instead of  $L_j$  describing the occupation site of hydrophobic part of peptide  $L_{\Phi,j}$  is used, which is a variable describing the hydrophilic peptide part occupation-site.

Finally the peptide-peptide interactions are characterised by the following Hamiltonian function:

$$H_{P-P}^{\Phi} = -\frac{\gamma_{\Phi}}{2} \sum_{\langle i,j \rangle} d_p L_{\Phi,i} L_{\Phi,j}. \tag{3.21}$$

Six classes of peptides were been used in simulations – each class possessed different hydrophobic length ( $d_p$ ) and different degree of hydrophobicity (characterized by  $\gamma_w$  and  $\gamma_{\Phi}$ ). Among these six classes three of them were analysed thoroughly and the results of simulations performed for temperature of the system  $T = 320$  K (above the phase transition of lipid used in this model) are presented in Fig. 24.

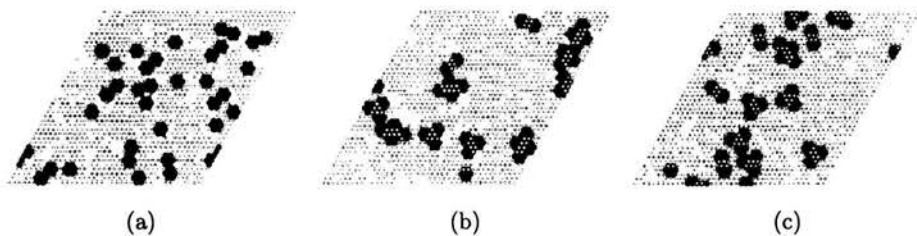


FIGURE 24. Snapshots of the microconfiguration of the lattice of dipalmitoylIPC-peptide mixtures for different values of peptide hydrophobic length ( $d_p$ ) and interaction parameters ( $\gamma_w$  and  $\gamma_{\Phi}$ ); after [27].

As can be seen in Fig. 24a completely hydrophobic peptides ( $\gamma_w = -\gamma$  and  $\gamma_{\Phi} = 0$ ) show no tendency to aggregate in lipid bilayer. Simulation

results show that the probability of finding peptide aggregates is very low. For partially hydrophilic peptides the tendency for aggregation depends on the values of the interaction parameters. For  $\gamma_w = 0$  and  $\gamma_\Phi = 3\gamma$ , (see Fig. 24b) peptide aggregates can be observed in membrane and probability of finding aggregate containing 3 peptide molecules is the biggest. Peptide clustering is even greater for molecules characterized by  $\gamma_w = 5\gamma$  and  $\gamma_\Phi = 5\gamma$ . As can be inferred from Fig. 24c peptides tend to aggregate by keeping their hydrophilic region in loose contact with hydrophilic regions of other peptides.

## References

1. M. AIELLO, O. MORAN, M. PISCIOTTA, F. GAMBALE, Interaction between dihydropyridines and phospholipid bilayers: a molecular dynamics simulation, *European Biophysical Journal*, Vol.27, pp.211-218, 1998.
2. Y. BARENHOLZ, Cholesterol and other membrane active sterols: from membrane evolution to "rafts", *Progress in Lipid Research*, Vol.41, No 1, pp.1-5, 2002.
3. P.R. CULLIS, B. DE KRUIJFF, Lipid polymorphism and the functional roles of lipids in biological membranes, *Biochimica et Biophysica Acta*, Vol.559, No 4, pp.399-420, 1979.
4. C. DIETRICH, L.A. BAGATOLLI, Z.N. VOLOVYK, N.L. THOMPSON, M. LEVI, K. JACOBSON, E. GRATTON, Lipid rafts reconstituted in model membranes, *Biophysical Journal*, Vol. 80, pp.1417-1428, 2001.
5. M. EDIDIN, Lipid microdomains in cell surface membranes, *Current Opinion in Structural Biology*, Vol.7, pp.528-532, 1997.
6. M. ENGELKE, R. JESSEL, A. WIECHMANN, H.A. DIEHL, Effect of inhalation anaesthetics on the phase behaviour, permeability and order of phosphatidylcholine bilayers, *Biophysical Chemistry*, Vol.67, pp.127-38, 1997.
7. J.M. FORD, Experimental reversal of P-glycoprotein-mediated multidrug resistance by pharmacological chemosensitisers, *European Journal of Cancer*, Vol.32A, pp.991-1001, 1996.
8. E. GORTER, F. GREDEL, On bimolecular layers of lipids on the chromocytes of the blood, *Journal of Experimental Medicine*, Vol. 41, pp.439-443, 1925.
9. H. HÄGERSTRAND, B. ISOMAA, Vesiculation induced by amphiphiles in erythrocytes, *Biochimica et Biophysica Acta*, Vol.982, pp.179-186, 1989.
10. T. HEIMBURG, Mechanical aspects of membrane thermodynamics. Estimation of mechanical properties of lipid membranes close to the chain melting transition from calorimetry, *Biochimica et Biophysica Acta*, Vol.1415, pp.147-162, 1998.
11. A.B. HENDRICH, O. WESOLOWSKA, K. MICHALAK, Trifluoperazine induces domain formation in zwitterionic phosphatidylcholine but not in charged phosphatidylglycerol bilayers, *Biochimica et Biophysica Acta*, Vol.1510, pp.414-425, 2001.
12. A.B. HENDRICH, K. MICHALAK, Lipids as a target for drugs modulating multidrug resistance of cancer cells, *Current Drug Targets*, Vol.4, pp.22-30, 2003.

13. N.M. HOOPER, Detergent-insoluble glycosphingolipid/cholesterol-rich membrane domains, lipid rafts and caveolae, *Molecular Membrane Biology*, V.16, pp.145-156, 1999.
14. N. JANES, Curvature stress and polymorphism in membranes, *Chemistry and Physics of Lipids*, Vol.81, pp.133-150, 1996.
15. J.A. KILLIAN, Hydrophobic mismatch between proteins and lipids in membranes, *Biochimica et Biophysica Acta*, Vol.1376, pp.401-416, 1998.
16. K. KOBAYASHI, S. MITTLER-NEHER S., J. SPINKE, G. WENZ, W. KNOLL, Translocation of alkali metal cations by lipophilic cyclodextrin derivatives through black lipid membranes, *Biochimica et Biophysica Acta*, Vol.1368, pp.35-40, 1998.
17. B. DE KRUIJFF., P.R. CULLIS, A.J. VERKLEIJ, M.J. HOPE, C.J.A. VAN ECHTELD, T.F. TARASCHI, P. VAN HOOGEVEST, J.A. KILLIAN, A. RIETVELD, A.T.M. VAN DER STEEN, Modulation of lipid polymorphism by lipid-protein interactions. in: *Progress in protein-lipid interactions*, J.J.H.H.M. de Pont and A. Watts, (Eds.), pp.89-142, Amsterdam, Elsevier 1985.
18. T.V. KURZCHALIA, R.G. PARTON, Membrane microdomains and caveolae, *Current Opinion in Cell Biology*, Vol. 11, pp.424-431, 1999.
19. R. N. MCELHANEY, Differential scanning calorimetric studies of lipid-protein interactions in model membrane systems, *Biochimica et Biophysica Acta*, Vol.864, pp.361-421, 1986.
20. P.B MOORE, C.F. LOPEZ, M.L. KLEIN, Dynamical properties of a hydrated lipid bilayer from a multianosecond molecular dynamics simulation, *Biophysical Journal*, Vol.81, pp.2484-2494, 2001.
21. D.A. PINK, J.G. GREEN, D. CHAPMAN, Raman scattering in bilayers of saturated phosphatidylcholines. Experiment and theory, *Biochemistry*, Vol.19, pp.349-356, 1980.
22. ROTHNIE, D. THERON, L. SOCENEANTU, C. BERRIDGE, M. TRAIKIA, G. BERRIDGE, C.F. HIGGINS, P.F. DEVAUX, R. CALLAGHAN, The importance of cholesterol in maintenance of P-glycoprotein activity and its membrane perturbing influence, *Biophysical Journal*, Vol.30, pp.430-442, 2001.
23. T. RÓG., M. PASENKIEWICZ-GIERULA, Cholesterol effects on the phosphatidylcholine bilayer nonpolar region: a molecular simulation study, *Biophysical Journal*, Vol.81, pp.2190-2202, 2001.
24. M.P. SHEETZ, S.J. SINGER, Biological membranes as bilayer couples. A molecular mechanism of drug-erythrocyte interactions, *Proceedings of the National Academy of Sciences USA*, Vol.71, pp.4457-4461, 1974.
25. K. SIMONS, E. IKONEN, Functional rafts in cell membranes, *Nature*, Vol.387, pp.569-572, 1997.
26. S.J. SINGER, G.L. NICOLSON, The fluid mosaic model of the structure of cell membranes, *Science*, Vol.175, pp.720-731, 1972.
27. M.M. SPEROTTO, A theoretical model for the association of amphiphilic transmembrane peptides in lipid bilayers, *European Biophys. J.*, Vol.26, 405-416, 1997.
28. S. SVETINA., B. ZEKS, Membrane bending energy and shape determination of phospholipid vesicles and red blood cells, *European Biophys. J.*, V.17, pp.101-111, 1989.

